

1  
2  
3  
4  
5  
6  
7  
8  
9  
10  
11  
12  
13  
14  
15  
16  
17  
18  
19  
20  
21  
22  
23

Multiple-source heterotrophy fueled by aged organic carbon in an  
urbanized estuary

David R. Griffith<sup>1</sup> and Peter A. Raymond

*Yale University, School of Forestry and Environmental Studies  
195 Prospect Street  
New Haven, Connecticut 06511  
davidgriffith@aya.yale.edu  
peter.raymond@yale.edu*

*Revised Marine Chemistry Manuscript (MARCHE-D-10-00003)  
Submitted in revised form August 2, 2010*

<sup>1</sup>Corresponding author, present address: Massachusetts Institute of Technology and Woods Hole  
Oceanographic Institution, Joint Program in Oceanography, MS#4, Woods Hole, MA  
02543, USA; telephone: 508-289-3396; fax: 508-457-2164; email: dgriffith@whoi.edu

24 **Abstract**

25           The lower Hudson River is a highly urbanized estuary that receives large inputs of treated  
26 wastewater. To determine how organic matter from wastewater influences carbon cycling in this  
27 type of system, we measured chlorophyll *a*, pCO<sub>2</sub>, dissolved organic carbon (DOC), δ<sup>13</sup>C-DOC,  
28 and Δ<sup>14</sup>C-DOC along the salinity gradient and at wastewater treatment plants. Isotopic mixing  
29 curves indicate a net removal of DOC that is <sup>13</sup>C enriched and <sup>14</sup>C depleted. The amount of DOC  
30 removed was consistent with CO<sub>2</sub> evasion from the estuary. During two transects at average to  
31 low flow, the lower Hudson River Estuary was a heterotrophic system with CO<sub>2</sub> evasion  
32 balanced by the utilization of aged DOC derived from wastewater and marine phytoplankton that  
33 enter the estuary at the seaward end-member. DOC removals were largest during a period of high  
34 river flow, when isotopic mixing curves also suggest large contributions from labile terrestrial  
35 OC sources. Overall, our results suggest that net heterotrophy in the lower Hudson River Estuary  
36 is fueled by aged labile DOC derived from a combination of sources, which are influenced by  
37 seasonal phytoplankton blooms, hydrological conditions, and the nature of wastewater inputs.

38

39

40

41

42 **Keywords**

43 Dissolved organic carbon; Wastewater; Sewage; Heterotrophy; <sup>13</sup>C; <sup>14</sup>C; Isotope mixing curves;  
44 Carbon dioxide; Chlorophyll; Carbon cycle; USA; Hudson River Estuary

45

46 **1. Introduction**

47 Estuaries are complex aquatic systems that link the terrestrial and ocean carbon cycles  
48 and can influence the amount and character of dissolved organic carbon (DOC) delivered to the  
49 coastal ocean. Within and across estuaries, DOC has variable composition, concentration,  
50 isotopic signature, and lability. DOC character is largely determined by its sources and the  
51 processes that transform it within rivers and estuaries (McCallister et al. 2006; Moran et al. 1999;  
52 Raymond et al. 2004).

53 Several major processes alter DOC as it travels through an estuary, including autotrophic  
54 additions (Cole and Caraco 2006; Peterson et al. 1994; Raymond and Bauer 2001a),  
55 heterotrophic removals (Howarth et al. 1996; Maranger et al. 2005; Taylor et al. 2003; Van den  
56 Meersche et al. 2009), photochemistry (Mopper and Kieber 2002), flocculation (Sholkovitz  
57 1978), and interactions with suspended particles (Hedges and Keil 1999; Servais and Garnier  
58 2006). Taken together, these processes have major implications for land-ocean carbon and  
59 nutrient fluxes and the global carbon cycle.

60 There are gaps in our understanding of how DOC is transformed within estuaries,  
61 especially in saline reaches surrounded by megacities. In highly urbanized estuaries, human  
62 wastewater can be a significant freshwater input that drives two competing processes with  
63 respect to an estuary's net metabolism and carbon cycling. In the first, nitrogen and phosphorus  
64 from wastewater can increase primary productivity leading to autochthonous organic carbon  
65 production (Howarth et al. 2006; Muylaert et al. 2000). Conversely, labile organic matter from  
66 wastewater can promote heterotrophic removal of organic carbon and subsequent production and  
67 release of CO<sub>2</sub>. Although most estuaries are generally supersaturated in CO<sub>2</sub> and release a large  
68 amount of carbon into the atmosphere (Borges et al. 2006; Cai and Wang 1998; Frankignoulle et

69 al. 1998), these fluxes can vary with water residence time and organic matter inputs. The effect  
70 of wastewater inputs on organic carbon dynamics and the autotrophic-heterotrophic balance in  
71 urbanized estuaries remains unclear and context dependent (Abril et al. 2002; Alvarez-Salgado  
72 and Miller 1998; Muylaert et al. 2005).

73 The Hudson River Estuary is a highly urbanized system that receives effluent from more  
74 than 100 wastewater treatment plants (WWTPs) and is home to ~ 8.5 million inhabitants.  
75 Previous studies of carbon dynamics in the saline, “lower” estuary are limited and have focused  
76 on primary and bacterial production (Howarth et al. 2006; Taylor et al. 2003). In contrast, work  
77 on the tidal freshwater section of the estuary has been more intense and indicates a strongly  
78 heterotrophic system driven by inputs of labile organic matter from aged terrestrial sources (Cole  
79 and Caraco 2001; del Giorgio and Pace 2008; Howarth et al. 1992; McCallister et al. 2004;  
80 Raymond and Bauer 2001c). These and other studies highlight the importance of internal DOC  
81 processing in estuaries (see Peterson et al. 1994).

82 The goal of the present study was to evaluate the effect of wastewater inputs on net  
83 carbon dynamics in a mega-city estuary by measuring  $p\text{CO}_2$ , chlorophyll *a*, DOC,  $\delta^{13}\text{C}$ -DOC,  
84 and  $\Delta^{14}\text{C}$ -DOC across a salinity gradient in the lower Hudson River Estuary.

85

## 86 **2. Methods**

### 87 ***2.1 Study site***

88 The Hudson River Estuary is tidal from New York City to Troy, NY (river kilometer  
89 240); the location of the salt front depends on river flow and tidal strength. Mean annual  
90 discharge at the southern tip of Manhattan is  $545 \text{ m}^3 \text{ s}^{-1}$  and varies between typical summertime  
91 low flows of  $200 \text{ m}^3 \text{ s}^{-1}$  and spring/fall freshets of  $2000 \text{ m}^3 \text{ s}^{-1}$ . In 2000, wastewater input into the

92 entire estuary was  $\sim 70 \text{ m}^3 \text{ s}^{-1}$  (80% of which derives from the New York City metropolitan  
93 area), representing a large percentage of the total summer flow of the Hudson (Brosnan et al.  
94 2006).

## 95 **2.2 Sampling**

96 Estuarine surface water was sampled along the Hudson River, from West Point to the  
97 Statue of Liberty, during three sampling cruises: 8 June 2005, 19 April 2006, and 18 July 2006  
98 (Fig. 1). On these days, Hudson River discharge was  $307 \text{ m}^3 \text{ s}^{-1}$ ,  $402 \text{ m}^3 \text{ s}^{-1}$ , and  $785 \text{ m}^3 \text{ s}^{-1}$   
99 respectively (Fig. 2; estimated as 167% of the discharge from the Green Island, NY river gauge  
100 (Howarth et al. 1996)). In August 2006, wastewater effluent was sampled from six representative  
101 WWTPs that were spread along the lower Hudson River Estuary (Fig. 1) and had average  
102 discharges ranging from 4.6 to 254 million gallons per day (MGD; Table 1).

103 During each estuarine transect,  $p\text{CO}_2$ , salinity, and chlorophyll *a* were measured  
104 continuously with an on-board flow-through system. Discrete water samples were also collected  
105 using  $^{14}\text{C}$ -clean techniques at 6 - 7 sites in acid-washed (1% HCl) polycarbonate bottles and  
106 immediately sub-sampled for subsequent laboratory measurements of DOC,  $\delta^{13}\text{C}$ -DOC,  $\Delta^{14}\text{C}$ -  
107 DOC, and chlorophyll *a*. All samples were transported to the lab on ice and then frozen (DOC)  
108 or refrigerated (chlorophyll *a*). WWTP effluent samples were collected at the outflow access  
109 points with dip bottles or dedicated sampling spigots (WWTP 3) and handled in the same way as  
110 the estuarine samples.

### 111 **2.2.1 Flow-through system ( $p\text{CO}_2$ , salinity, chlorophyll *a*)**

112 The on-board flow-through system was configured as follows: a YSI 600XLM Sonde  
113 probe that measured salinity was connected in series to a chlorophyll *a* probe (“WET Labs  
114 WETStar Chlorophyll Fluorometer”) and a  $\text{CO}_2$  shower head equilibrator (Raymond and

115 Hopkinson 2003). Each probe was attached to a data logger that took readings and global  
116 positioning system (GPS) coordinates every second.

### 117 *2.2.2 Chlorophyll a calibration*

118 Laboratory measurements of chlorophyll *a* were used to calibrate the flow-through  
119 chlorophyll *a* probe. Refrigerated sub-samples were passed through baked GFF filters under low  
120 light conditions within 24 hours of returning to the lab. Each filter was then wrapped in baked  
121 foil and frozen. At a later date, chlorophyll *a* concentrations were measured fluorometrically  
122 after a 24-hour acetone extraction. Reported concentrations have been corrected for chlorophyll  
123 *a* degradation products (Environmental Protection Agency Method 445.0).

### 124 *2.2.3 DOC, $\delta^{13}\text{C}$ -DOC, $\Delta^{14}\text{C}$ -DOC*

125 In the field, DOC sub-samples were passed through a 1.0  $\mu\text{m}$  combusted QMA filter and  
126 collected in 125 mL acid-washed polycarbonate bottles. Upon returning to the lab, DOC  
127 samples were acidified to pH  $\sim$  2.5 with 1 mL of 60% phosphoric acid and frozen. The entire 125  
128 mL sample was placed in a quartz reaction tube and converted to  $\text{CO}_2$  by high-energy UV  
129 irradiation (2400 W; see Williams and Gordon 1970) followed by purification and collection on  
130 a gas extraction line (Bauer et al. 1992; Raymond and Bauer 2001a). DOC concentrations and  
131 recoveries were determined using a calibrated Baratron absolute pressure gauge to measure  $\text{CO}_2$   
132 pressure. The sample was then isolated in a glass ampoule to await  $\delta^{13}\text{C}$  and  $\Delta^{14}\text{C}$  analysis.

### 133 *2.3 Analytical methods*

134  $\delta^{13}\text{C}$ -DOC measurements were made at the National Ocean Sciences Accelerator Mass  
135 Spectrometry Facility (NOSAMS) and the National Science Foundation-University of Arizona  
136 Accelerator Mass Spectrometry Facility (NSF-Arizona AMS) by mass spectral analysis of  $\text{CO}_2$   
137 gas previously purified on a gas extraction line at Yale University. Natural  $^{14}\text{C}$  sampling and

138 analysis required meticulous attention to detail to avoid contamination (e.g., all bottles, filtration  
139 apparatuses, forceps, etc. were appropriately cleaned, acidified, or baked).  $\Delta^{14}\text{C}$ -DOC  
140 measurements took place at NOSAMS (June and April transects) and NSF-Arizona AMS (July  
141 transect and WWTPs). At each facility, purified  $\text{CO}_2$  from each sample was catalytically  
142 converted to graphite (McNichol et al. 1992; Vogel et al. 1987) and pressed into a target that was  
143 run on an accelerator mass spectrometer. Total measurement uncertainty for the  $\Delta^{14}\text{C}$  analyses of  
144 these samples is  $\sim 5 - 7\%$ . Radiocarbon ages are reported according to Stuiver and Polach (1977)  
145 and Stuiver (1980).

#### 146 **2.4 Isotope Mixing Curves**

147 Isotope mixing models are valuable and sensitive tools for assessing elemental cycling in  
148 estuaries. Specifically, a dual isotope mixing approach using both  $^{14}\text{C}$  and  $^{13}\text{C}$  has been  
149 successful at resolving the source and age of organic matter in aquatic systems (McCallister et al.  
150 2004; Raymond and Bauer 2001b; Spiker 1980). Isotope mixing curves use salinity as a  
151 conservative tracer and require that both the total DOC concentration and isotopic composition  
152 ( $I$ ) of the riverine ( $riv$ ) and high-salinity/marine ( $mar$ ) end-members are known. The  
153 conservative isotope value ( $\delta^{13}\text{C}$  or  $\Delta^{14}\text{C}$ ) for a sample at a known salinity ( $I_s$ ) is then calculated  
154 as:

$$155 \quad I_s = \frac{(f_{riv} I_{riv} DOC_{riv} + (1 - f_{riv}) I_{mar} DOC_{mar})}{DOC_{mix}} \quad (1)$$

156 where the riverine fraction,  $f_{riv}$ , is calculated from salinity, and  $DOC_{mix}$  is the amount of DOC  
157 expected from conservative mixing of the freshwater and marine end-members. A conservative  
158 mixing curve is drawn by evaluating  $I_s$  across the relevant salinity range (see Fig. 3). If actual  
159 isotope values differ from the conservative mixing curve, one concludes that processes apart  
160 from simple end-member mixing are at work (see Cifuentes and Eldridge 1998). As an example,

161 consider an estuary where measured  $\Delta^{14}\text{C}$ -DOC values lie below (are depleted relative to) the  
162 conservative curve. This could be interpreted as a net addition of  $^{14}\text{C}$  depleted DOC and/or  
163 removal of  $^{14}\text{C}$  enriched DOC.

164 The two end-member mixing model described above assumes no major inputs of fresh  
165 water along the estuarine study site. In our case, this is a good assumption as tributary inputs are  
166 minor and most WWTP effluent is discharged outside of our study area. The mixing model also  
167 assumes that the composition of each end-member is invariant on timescales of estuarine mixing.

## 168 ***2.5 Estimates of net DOC removal***

169 Measured DOC concentrations were plotted as a function of salinity and fit with simple  
170 quadratic equations to estimate net DOC removals along each transect using the method of Kaul  
171 and Froelich (1984). The internal flux (input or removal) of DOC is defined as

$$172 \quad \text{Internal flux} = Q(C_s - C_o) \quad (2)$$

173 where  $Q$  is freshwater flow,  $C_o$  is the concentration at zero salinity, and  $C_s$  is the concentration  
174 where the tangent of the quadratic equation at the saline end-member intercepts the y-axis (at  
175 zero salinity). Raymond and Bauer (2001a) describe this method in detail.

## 176 ***2.6 Gas exchange estimates***

177 Rough estimates of  $\text{CO}_2$  exchange between water and atmosphere were calculated using  
178 average  $\text{pCO}_2$  values for each transect and a gas exchange coefficient ( $k$ ) of  $5 \pm 1 \text{ cm h}^{-1}$ . This  
179 particular  $k$  was chosen because it lies in the middle of the predicted range ( $3 - 7 \text{ cm h}^{-1}$ ) for  
180 estuaries and rivers such as the Hudson (Raymond and Cole 2001) and also agrees well with  
181 field and empirical studies of gas exchange in the freshwater tidal Hudson River at average wind  
182 speeds and tidal velocities (Clark et al. 1994; Raymond and Cole 2001; Ho et al. 2002; Zappa et  
183 al. 2007).

184

### 185 **3. Results**

#### 186 **3.1 DOC mixing curves**

187 Results for all three transects indicate that DOC concentrations were highest at the  
188 freshwater end member and decreased non-conservatively towards the saline end member,  
189 indicating net removal of DOC (Fig. 3a). Using Eq. 2 and the method of Kaul and Froelich  
190 (1984), we estimate internal DOC removal fluxes of  $22 \text{ mmol C m}^{-2} \text{ d}^{-1}$ ,  $35 \text{ mmol C m}^{-2} \text{ d}^{-1}$ , and  
191  $72 \text{ mmol C m}^{-2} \text{ d}^{-1}$  for the June 2005, April 2006, and July 2006 transects respectively. The  $\delta^{13}\text{C}$ -  
192 DOC and  $\Delta^{14}\text{C}$ -DOC isotope mixing curves also exhibit non-conservative behavior with depleted  
193  $\delta^{13}\text{C}$ -DOC values (Fig. 3b) and enriched  $\Delta^{14}\text{C}$ -DOC values (Fig. 3c) relative to the conservative  
194 mixing curves.

#### 195 **3.2 Wastewater**

196 WWTP effluent had similar characteristics despite differences in location, source water,  
197 and outflow (Fig. 1; Table 1). On average, effluent DOC had a concentration of  $954 \pm 306 \text{ }\mu\text{M}$   
198 (SD), a  $\delta^{13}\text{C}$  value of  $-26.6 \pm 1.1\text{‰}$  (SD), and a  $\Delta^{14}\text{C}$  value of  $-163.5 \pm 24.4\text{‰}$  (SD) (Griffith et  
199 al. 2009). The latter corresponds to an average wastewater  $^{14}\text{C}$ -DOC age of 1379 years BP  
200 (Table 1). Using a conservative estimate of wastewater discharge into the lower Hudson ( $60 \text{ m}^3$   
201  $\text{s}^{-1}$ ) we estimate that the total DOC input from wastewater is  $33 \text{ mmol C m}^{-2} \text{ d}^{-1}$ . Most WWTPs  
202 are required to measure biological oxygen demand (BOD; a proxy for labile carbon) in the  
203 effluent on a regular basis. For the six WWTPs we sampled, average BOD (5 day;  $20 \text{ }^\circ\text{C}$ ) varied  
204 by 18 - 37% between June 2005 and July 2006 (EPA Envirofacts database;  
205 [http://oaspub.epa.gov/enviro/ef\\_home2.water](http://oaspub.epa.gov/enviro/ef_home2.water)). It is noteworthy that most of the wastewater

206 entering our study area is actually discharged from WWTPs on the East River and in New York  
207 Harbor then pushed northwards into the estuary by tides.

### 208 **3.3 *pCO<sub>2</sub>* and chlorophyll *a***

209 *pCO<sub>2</sub>* and chlorophyll *a* data for each transect are presented in Figs. 4a and 4b  
210 respectively. Comparisons of *pCO<sub>2</sub>* and chlorophyll *a* averages and ranges are shown in Table 2.  
211 Mean *pCO<sub>2</sub>* values of 1000  $\mu\text{atm}$ , 670  $\mu\text{atm}$ , and 2059  $\mu\text{atm}$  (for June, April, and July transects  
212 respectively) are all above atmospheric saturation (380  $\mu\text{atm}$ ). Therefore, in all three cruises the  
213 estuary was a net source of  $\text{CO}_2$  to the atmosphere. Generally, *pCO<sub>2</sub>* was highest near the north  
214 end of Haverstraw Bay (river km 65), decreased to a local minima at the south end of Haverstraw  
215 Bay (river km 35), then increased along the length of Manhattan before declining sharply in NY  
216 Harbor (Fig. 4a). The June 2005 transect was the only one to exhibit a reach of sub-atmospheric  
217 *pCO<sub>2</sub>* values ( $<380 \mu\text{atm}$ ). Using a gas exchange coefficient of  $5 \pm 1 \text{ cm h}^{-1}$  (Clark et al. 1994;  
218 Raymond and Cole 2001; Ho et al. 2002; Zappa et al. 2007) and mean *pCO<sub>2</sub>* values for each  
219 transect, we estimate  $\text{CO}_2$  effluxes of  $23 \pm 5 \text{ mmol C m}^{-2} \text{ d}^{-1}$ ,  $11 \pm 2 \text{ mmol C m}^{-2} \text{ d}^{-1}$ , and  $61 \pm 12$   
220  $\text{mmol C m}^{-2} \text{ d}^{-1}$  (June, April, and July respectively).

221 A relationship between the chlorophyll *a* probe and laboratory-based fluorometric  
222 chlorophyll *a* measurements (Fig. 5) allowed us to convert probe voltages into chlorophyll *a*  
223 concentrations at high temporal resolution. In the April 2006 transect, chlorophyll *a*  
224 concentrations were highest at the freshwater and saline extremes (Fig. 4b). Chlorophyll *a*  
225 concentrations were significantly higher throughout the July 2006 transect and displayed a sharp  
226 peak at the south end of Haverstraw Bay (river km 40; Fig. 4b). In the June 2005 transect,  
227 chlorophyll *a* is low in Haverstraw Bay but displays several sharp downstream peaks (river km

228 10 - 35). Chlorophyll *a* data from the June 2005 transect were measured with the same probe and  
229 corrected using the relationship derived from the April and July 2006 transects (Fig. 5).

230

## 231 **4. Discussion**

### 232 **4.1 *pCO<sub>2</sub>* and chlorophyll *a***

233 Our study suggests that the saline Hudson River Estuary is less supersaturated in CO<sub>2</sub>  
234 than many other large rivers and estuaries around the world (Cole and Caraco 2001;  
235 Frankignoulle 1998; Raymond et al. 2000), a surprising result given large sewage treatment plant  
236 loadings. Still, our pCO<sub>2</sub> data suggest that the lower Hudson is a net heterotrophic system (Fig.  
237 4a). This finding is consistent with several previous studies (Howarth et al. 2006; Taylor et al.  
238 2003) but estimates of the magnitude vary. Our estimate of metabolism is consistent with long-  
239 term studies in the tidal, freshwater Hudson (Cole and Caraco 2001; Raymond et al. 1997), but  
240 differ markedly from those of Taylor et al. (2003). Based on bottle incubations, the latter  
241 reported average dissolved inorganic carbon (DIC) production rates of 330 mmol C m<sup>-2</sup> d<sup>-1</sup> in the  
242 saline Hudson. In our study, pCO<sub>2</sub> was between 300 μatm and 2434 μatm. Using a gas exchange  
243 coefficient of 5 cm h<sup>-1</sup> (Clark et al. 1994; Raymond and Cole 2001; Ho et al. 2002; Zappa et al.  
244 2007), we calculate a maximum air-water flux of ~ 90 mmol C m<sup>-2</sup> d<sup>-1</sup>, or about ¼ of the flux  
245 reported by Taylor et al. (2003). This discrepancy could be due to problems with scaling bottle  
246 incubations, a lack of seasonal pCO<sub>2</sub> data, or a large export of carbonate alkalinity from the  
247 Hudson.

248 It is likely that several processes determine the spatial patterns observed in our pCO<sub>2</sub> data  
249 (Fig. 4a). Respiration drives pCO<sub>2</sub> increases but is counteracted by primary production and gas  
250 exchange in supersaturated estuaries (Borges et al. 2006). Carbon dioxide concentrations may

251 also change along salinity gradients due to mixing of buffered seawater with freshwater.  
252 Turbidity maxima may be sites of in situ DOC production (Alvarez-Salgado and Miller 1998)  
253 and enhanced organic matter oxidation by bacteria attached to suspended particles (Servais and  
254 Garnier 2006; Uncles et al. 2000). In the Hudson, pCO<sub>2</sub> maxima were observed near turbidity  
255 maxima (near the top of Haverstraw Bay and at the George Washington Bridge) where bacterial  
256 respiration may be high and primary production is limited by a low photic zone to mixed layer  
257 depth ratio (Cole et al. 1992).

258         Generally, chlorophyll *a* and pCO<sub>2</sub> trends were inversely related (Figs. 4a and 4b). Yet  
259 the large localized chlorophyll *a* peak in July 2006 was not accompanied by significantly lower  
260 pCO<sub>2</sub> values. If excess chlorophyll is produced in the shoals and exported to the main stem of the  
261 Hudson, these results suggest a possible decoupling of the effect of shoal primary production on  
262 main stem CO<sub>2</sub> and O<sub>2</sub> dynamics. The observation that chlorophyll *a* concentrations and  
263 freshwater discharge were both at their highest during the July 2006 transect suggests an  
264 alternative explanation. Given that pCO<sub>2</sub> levels were also high during this transect, it seems  
265 likely that elevated chlorophyll *a* concentrations were due in part to primary production in the  
266 tidal freshwater Hudson followed by downstream transport into our study site.

#### 267 ***4.2 DOC dynamics***

268         Studies have shown that DOC behavior varies widely between estuaries (Abril et al.  
269 2002; Middelburg and Herman 2007; Peterson et al. 1994). For example, conservative mixing of  
270 DOC has been documented in the Humber (Alvarez-Salgado and Miller 1998), Rhine, Thames,  
271 Elbe, Douro (Abril et al. 2002; Middelburg and Herman 2007), and Columbia (Prahl and Coble  
272 1994). Net additions of DOC characterize the York (Raymond and Bauer 2001a), Betsiboka  
273 (Ralison et al. 2008), Gironde, Sado, Loire, and Ems (Abril et al. 2002; Middelburg and Herman

274 2007), while net removals have been observed in the highly urbanized Scheldt (Abril et al.  
275 2002). Recent studies in the Mississippi, Tyne, Tweed, and Pawcatuck River estuaries also  
276 suggest that DOC dynamics vary with the season and hydrological regime (McKenna 2004;  
277 Spencer et al. 2007; Wang et al. 2004).

278 DOC mixing curves for the lower Hudson Estuary indicate a net removal of DOC (22,  
279 35, and 72 mmol C m<sup>-2</sup> d<sup>-1</sup>; Fig. 3a). One reason to expect net removals is the low potential for  
280 autochthonous production in the lower Hudson. Phytoplankton and tidal marshes are important  
281 sources of DOC (Baines and Pace 1991; Peterson et al. 1994; Raymond and Hopkinson 2003),  
282 yet the lower estuary has very small spatial coverage of marshes and phytoplankton are generally  
283 still light limited (Cole and Caraco 2006). These observations are consistent with a net removal  
284 of DOC. The net DOC removal rates are similar to pCO<sub>2</sub> efflux estimates (23 ± 5, 11 ± 2, and 61  
285 ± 12 mmol C m<sup>-2</sup> d<sup>-1</sup>; Fig. 4a) despite uncertainties associated with quadratic curve fitting and the  
286 use of average pCO<sub>2</sub> and gas transfer velocity values. The general agreement between the DOC  
287 removals and pCO<sub>2</sub> efflux estimates, coupled with low primary production, are consistent with a  
288 net heterotrophic system in which evasion is balanced partly by DOC consumption by bacteria.

289 Potential sources of allochthonous labile DOC that could drive net DOC removals and  
290 CO<sub>2</sub> evasion include riverine DOC, wastewater DOC, saltmarsh DOC from the Raritan, Passaic,  
291 and Hackensack drainages, and DOC from primary production in NY harbor and the coastal  
292 ocean. A recent study concluded that most of the labile riverine OC delivered to the Hudson  
293 River Estuary is utilized near Troy (river km 240), leaving behind generally refractory DOC that  
294 is then transported conservatively through the tidal freshwater Hudson (del Giorgio and Pace  
295 2008). The amount of wastewater DOC that enters the saline Hudson (mostly released outside of  
296 our study area and subsequently pushed in by tides) is on the same order as estimates of DOC

297 removal and pCO<sub>2</sub> efflux. The amount of marine OC advected into the lower Hudson is difficult  
298 to quantify but remains a potentially large source of labile OC. Below we use dual isotope  
299 mixing curves to further constrain possible sources of labile DOC.

#### 300 *4.3 $\delta^{13}\text{C}$ -DOC and $\Delta^{14}\text{C}$ -DOC dynamics*

301 In the lower Hudson,  $\delta^{13}\text{C}$ -DOC values were depleted and  $\Delta^{14}\text{C}$ -DOC values were  
302 enriched relative to their respective conservative mixing curves (Figs. 3b and 3c). Together with  
303 evidence of net DOC removal (from both mixing curves and pCO<sub>2</sub> levels), the isotope data  
304 generally suggest removal of a DOC pool that is <sup>13</sup>C enriched and <sup>14</sup>C depleted. When the  
305 method of Kaul and Froelich (1984) was applied using quadratic fits to <sup>12</sup>C, <sup>13</sup>C, and <sup>14</sup>C  
306 concentrations individually ( $R^2 = 0.97$ ), it was possible to quantify the net isotopic signature of  
307 the DOC pool that was removed in the lower Hudson during the June transect. This labile DOC  
308 pool was enriched in <sup>13</sup>C ( $\delta^{13}\text{C} = -20\text{‰}$ ) and depleted in <sup>14</sup>C ( $\Delta^{14}\text{C} = -232\text{‰}$ ).

309 Three major sources of labile DOC having enriched <sup>13</sup>C and depleted <sup>14</sup>C signatures are  
310 autochthonous estuarine DOC, allochthonous marine DOC, and wastewater DOC. Our  
311 chlorophyll *a* data and previous estimates of near zero net ecosystem production (Baines and  
312 Pace 1991; Swaney et al. 1999) suggest that the amount of DOC derived from autochthonous  
313 production within the lower Hudson will be small. Wastewater ( $\delta^{13}\text{C} = -26.6\text{‰}$  and  $\Delta^{14}\text{C} = -$   
314  $163.5\text{‰}$  (Table 1)) and marine phytoplankton ( $\delta^{13}\text{C} \sim -20\text{‰}$  and  $\Delta^{14}\text{C} \sim -50\text{‰}$ ) are both large  
315 potential sources of labile DOM that are enriched in <sup>13</sup>C and depleted in <sup>14</sup>C relative to our  
316 mixing curves (Figs. 3b and 3c). However, the  $\delta^{13}\text{C}$  value of the removed DOC pool in June (-  
317  $20\text{‰}$ ) points to a marine or C<sub>4</sub>-derived OC source (Currin et al. 1995) while the  $\Delta^{14}\text{C}$  value (-  
318  $232\text{‰}$ ) is much closer to the wastewater OC source. In fact, the pool of removed DOC is even  
319 more depleted in <sup>14</sup>C (i.e., older) than both wastewater and marine OC, suggesting significant

320 contributions from a component of highly aged DOC. One possible source is particle bound  
321 terrestrial OC that has been mobilized or desorbed within the estuary (Alvarez-Salgado and  
322 Miller 1998; McCallister et al. 2004). Another possibility is wastewater OC derived from  
323 petrochemicals ( $\Delta^{14}\text{C} = -1000\text{‰}$ ), such as surfactants, pharmaceuticals, and personal care  
324 products (Griffith et al. 2009). Removing even small amounts of highly aged DOC could help  
325 explain the  $\Delta^{14}\text{C}$  value of the removed DOC pool ( $-232\text{‰}$ ). Furthermore, although the  $^{13}\text{C}$   
326 signature of removed DOC ( $-20\text{‰}$ ) is not consistent with the removal of only  $\text{C}_3$ /petroleum ( $\sim$  -  
327  $28\text{‰}$ ), wastewater organic matter also has a large contribution of  $\text{C}_4$  ( $\sim$   $-12\text{‰}$ ) OC from crops  
328 (such as corn and sugar cane) that are potentially labile and highly  $^{13}\text{C}$ -enriched.

329 In general, OC from wastewater and fresh marine phytoplankton is easily biodegraded  
330 (Baines and Pace 1991; Servais et al. 1995). Thus, the contribution of each source to net DOC  
331 removal should depend on the relative magnitude of their inputs. In the saline Hudson we  
332 hypothesize that allochthonous wastewater DOC is utilized by bacteria throughout the year,  
333 supplemented by labile DOC from seasonal phytoplankton blooms in the New York Bight (see  
334 Malone 1977). Thus, an interesting feature of the Hudson River Estuary is that both of these  
335 labile sources of DOC are brought into the estuary from the seaward end-member through tidal  
336 mixing, as opposed to many other estuaries where the major source of labile DOC is from the  
337 riverine end-member. Thus, at times the saline Hudson River Estuary operates as an “upside-  
338 down estuary,” fueled by labile DOC from the seaward end-member.

339 Our July 2006 transect also suggests that removal of labile riverine DOC may increase  
340 during periods of high river discharge. Both discharge (USGS; Fig. 2) and net DOC removal  
341 were the largest for the July transect. The corresponding mixing curves suggest removal of  $^{14}\text{C}$ -  
342 depleted OC, but show mostly conservative  $^{13}\text{C}$  behavior (Figs. 3b and 3c). We attribute this to

343 an increased utilization of pre-aged and  $^{13}\text{C}$ -depleted riverine OC, which balances a concurrent  
344 removal of  $^{13}\text{C}$ -enriched OC from wastewater and marine phytoplankton. Other sources of  
345 uncertainty include groundwater DOC flux and the effect of combined sewage overflows (CSOs)  
346 and raw sewage releases, which also become more frequent during rainy periods and probably  
347 contain highly labile DOC.

348         Using a multiple-isotope approach on bacterial nucleic acids in the York and Hudson  
349 River estuaries, McCallister et al. (2004) concluded that bacteria are utilizing “old” ( $^{14}\text{C}$   
350 depleted) carbon derived from petroleum hydrocarbons or terrigenous sources that became labile  
351 after dissociation from mineral particles or photolysis and degradation of humic compounds.  
352 Recently, Hood et al. (2009) found that the lability of DOM in glacial watersheds was positively  
353 correlated with the  $^{14}\text{C}$  age of DOC. The present study suggests that “old” DOC derived from  
354 wastewater and marine phytoplankton are important sources of labile carbon to the saline  
355 Hudson River Estuary during periods of low to average river flow. Together, these studies  
356 suggest that “old” does not necessarily mean “refractory.”

357

## 358 **5. Conclusion**

359         Although the saline Hudson River Estuary is a net heterotrophic system that receives  
360 large wastewater inputs, we find lower  $\text{pCO}_2$  levels than previously reported for several  
361 urbanized European estuaries (Frankignoulle 1998). The reasons for this discrepancy are unclear,  
362 but may have to do with differences in estuary geomorphology, bacterial assemblages, or  
363 wastewater organic carbon character and concentration. Isotope mixing curves point towards the  
364 utilization of aged DOC derived from wastewater and/or marine phytoplankton, with potential  
365 contributions from labile riverine OC during high river discharge.

366

367 **Acknowledgments**

368 We are indebted to K. Mull, D. Butman, D. Barrowman, R. Kirschkel, W. Fitzgerald, B. Jersey,  
369 B. McKenna, B. Murak, and B. Ranheim for their help with this research project. G. Olack  
370 assisted with isotope analysis at the Yale Center for Stable Isotopic Studies. A. Leonard, R. Cruz,  
371 and A. Carey assisted with radiocarbon analyses at the NSF-Arizona AMS Facility. NOSAMS  
372 also provided radiocarbon measurements. This research was funded by the Hudson River  
373 Foundation's Tibor T. Polgar Fellowship, the Carpenter-Sperry Fund at Yale University, and the  
374 NSF-Arizona AMS Facility's Student Internship program.

375 **References**

- 376 Abril, G., M. Nogueira, H. Etcheber, G. Cabecadas, E. Lemaire, and M. J. Brogueira. 2002.  
377 Behavior of organic carbon in nine contrasting European estuaries. *Estuarine Coastal and*  
378 *Shelf Science* **54**: 241-262.
- 379 Alvarez-Salgado, X. A., and A. E. J. Miller. 1998. Dissolved organic carbon in a large  
380 macrotidal estuary (the Humber, UK): behavior during estuarine mixing. *Marine*  
381 *Pollution Bulletin* **37**: 216-224.
- 382 Baines, S. B., and M. L. Pace 1991. The production of dissolved organic matter by  
383 phytoplankton and its importance to bacteria – patterns across marine and fresh-water  
384 systems. *Limnology and Oceanography* **36**: 1078-1090.
- 385 Bauer, J. E., P. M. Williams, and E. R. M. Druffel. 1992. C-14 activity of dissolved organic-  
386 carbon fractions in the North-Central Pacific and Sargasso Sea. *Nature* **357**: 667-670.
- 387 Borges, A. V., L. S. Schiettecatte, G. Abril, B. Delille, and F. Gazeau. 2006. Carbon dioxide in  
388 European coastal waters. *Estuarine, Coastal and Shelf Science* **70**: 375-387.
- 389 Brosnan, T. M., A. Stoddard, and L. J. Hetling. 2006. Hudson River sewage inputs and impacts:  
390 past and present, p. 335-348. *In* J. S. Levinton and J. R. Waldman (eds.), *The Hudson*  
391 *River Estuary*. Cambridge University Press, New York.
- 392 Cai, W. J., and Y. Wang. 1998. The chemistry, fluxes, and sources of carbon dioxide in the  
393 estuarine waters of the Satilla and Altamaha Rivers, Georgia. *Limnology and*  
394 *Oceanography* **43**: 657-668.
- 395 Cifuentes, L. A., and P. M. Eldridge. 1998. A mass- and isotope-balance model of DOC mixing  
396 in estuaries. *Limnology and Oceanography* **43**: 1872-1882.

397 Clark, J.F., R. Wanninkhof, P. Schlosser, and H.J. Simpson. 1994. Gas exchange rates in the  
398 tidal Hudson River using a dual tracer technique. *Tellus* **46**: 274-285

399 Cole, J. J., and N. F. Caraco. 2001. Carbon in catchments: connecting terrestrial carbon losses  
400 with aquatic metabolism. *Marine and Freshwater Research* **52**: 101-110.

401 Cole, J. J., and N. F. Caraco. 2006. Primary production and its regulation in the tidal-freshwater  
402 Hudson River, p. 107-120. *In* J. S. Levinton and J. R. Waldman (eds.), *The Hudson River*  
403 *Estuary*. Cambridge University Press, New York.

404 Cole, J. J., N. F. Caraco, and B. L. Peierls. 1992. Can phytoplankton maintain a positive carbon  
405 balance in a turbid, freshwater, tidal estuary? *Limnology and Oceanography* **37**: 1608-  
406 1617.

407 Currin, C.A., S. Y. Newell, and H. W. Pearl. 1995. The role of standing dead *Spartina*  
408 *alterniflora* and benthic microalgae in saltmarsh food webs - considerations based on  
409 multiple stable isotope analysis. *Marine Ecology-Progress Series*, **121**: 99-116.

410 del Giorgio, P. A., and M. L. Pace. 2008. Relative independence of dissolved organic carbon  
411 transport and processing in a large temperate river: The Hudson River as both pipe and  
412 reactor. *Limnology and Oceanography* **53**: 185-197.

413 Frankignoulle, M., G. Abril, A. Borges, I. Bourge, C. Canon, B. Delille, E. Libert, and J-M.  
414 Theate. 1998. Carbon dioxide emission from European estuaries. *Science* **282**: 434-436.

415 Griffith, D. R., B. T. Barnes, and P. A. Raymond. 2009. Inputs of fossil carbon from wastewater  
416 treatment plants to U.S. rivers and oceans. *Environmental Science & Technology* **43**:  
417 5647-5651, doi:10.1021/es9004043.

418 Hedges, J. I., and R. G. Keil. 1999. Organic geochemical perspectives on estuarine processes:  
419 sorption reactions and consequences. *Marine Chemistry* **65**: 55-65.

420 Ho, D. T., P. Schlosser, and T. Caplow. 2002. Determination of longitudinal dispersion  
421 coefficient and net advection in the tidal Hudson River with a large-scale, high resolution  
422 SF6 tracer release experiment. *Environmental Science & Technology* **36**: 3234-3241.

423 Hood, E., J. Fellman, R. G. M. Spencer, P. J. Hernes, R. Edwards, D. D'Amore, et al. 2009.  
424 Glaciers as a source of ancient and labile organic matter to the marine environment.  
425 *Nature* **462**: 1044-1048, doi:10.1038/nature08580.

426 Howarth, R. W., R. Marino, D. P. Swaney, and E. W. Boyer. 2006. Wastewater and watershed  
427 influences on primary productivity and oxygen dynamics in the lower Hudson River  
428 Estuary, p. 121-139. *In* J. S. Levinton and J. R. Waldman (eds.), *The Hudson River*  
429 *Estuary*. Cambridge University Press, New York.

430 Howarth, R. W., R. Marino, R. Garritt, and D. Sherman. 1992. Ecosystem respiration and  
431 organic carbon processing in a large, tidally influenced river: the Hudson River.  
432 *Biogeochemistry* **16**: 83-102.

433 Howarth, R. W., R. Schneider, and D. Swaney. 1996. Metabolism and organic carbon fluxes in  
434 the tidal freshwater Hudson River. *Estuaries* **19**: 848-865.

435 Howarth, R.W., R. Marino, D.P. Swaney, and E.W. Boyer. 2006. Wastewater and watershed  
436 influences on primary productivity and oxygen dynamics in the lower Hudson River  
437 estuary, p. 121-139. *In* J.S. Levinton and J.R. Waldman (eds.), *The Hudson River*  
438 *Estuary*. Cambridge University Press, New York

439 Kaul, L. W., and P. N. Froelich, Jr. 1984. Modeling estuarine nutrient geochemistry in a simple  
440 system. *Geochimica et Cosmochimica Acta* **48**: 1417-1433.

441 Malone, T. C. 1977. Environmental regulation of phytoplankton productivity in the lower  
442 Hudson estuary. *Estuarine and Coastal Marine Science* **5**: 157-171.

- 443 Maranger, R. J., M. L. Pace, P. A. del Giorgio, N. F. Caraco, and J. J. Cole. 2005. Longitudinal  
444 spatial patterns of bacterial production and respiration in a large river-estuary:  
445 implications for ecosystem carbon consumption. *Ecosystems* **8**: 318-330.
- 446 McCallister, S. L., J. E. Bauer, H. W. Ducklow, and E. A. Canuel. 2006. Sources of estuarine  
447 dissolved and particulate organic matter: a multi-tracer approach. *Organic Geochemistry*  
448 **37**: 454-468.
- 449 McCallister, S. L., J. E. Bauer, J. E. Cherrier, and H. W. Ducklow. 2004. Assessing sources and  
450 ages of organic matter supporting river and estuarine bacterial production: a multiple-  
451 isotope approach. *Limnology and Oceanography* **49**: 1687-1702.
- 452 McKenna, J. H. 2004. DOC dynamics in a small temperate estuary: simultaneous addition and  
453 removal processes and implications on observed nonconservative behavior. *Estuaries* **27**:  
454 604-616.
- 455 McNichol, A. P., A. R. Gagnon, G. A. Jones, and E. A. Osborne. 1992. Illumination of a black  
456 box - analysis of gas composition during graphite target preparation. *Radiocarbon* **34**:  
457 321-329.
- 458 Middelburg, J. J., and P. M. J. Herman. 2007. Organic matter processing in tidal estuaries.  
459 *Marine Chemistry* **106**: 127-147.
- 460 Mopper, K., and D. J. Kieber. 2002. Photochemistry and cycling of carbon, sulfur, nitrogen, and  
461 phosphorus, p. 455-507. *In* D. A. Hansell and C. A. Carlson (eds.), *Biogeochemistry of*  
462 *marine dissolved organic matter*. Academic Press, San Diego, CA.
- 463 Moran, M. A., W. M. Sheldon, and J. E. Sheldon. 1999. Biodegradation of riverine dissolved  
464 organic carbon in five estuaries of the southeastern United States. *Estuaries* **22**: 55-64.

465 Muylaert, K., K. Sabbe, and W. Vyverman. 2000. Spatial and temporal dynamics of  
466 phytoplankton communities in a freshwater tidal estuary (Schelde, Belgium). *Estuarine*  
467 *Coastal and Shelf Science* 50:673-87

468 Muylaert, K., R. Dasseville, L. DeBrabandere, F. Dehairs, and W. Vyverman. 2005. Dissolved  
469 organic carbon in the freshwater tidal reaches of the Schelde estuary. *Estuarine Coastal*  
470 *and Shelf Science* **64**: 591-600.

471 Peterson, B., B. Fry, M. Hullar, S. Saupe, and R. Wright. 1994. The distribution and stable  
472 carbon isotopic composition of dissolved organic carbon in estuaries. *Estuaries* **17**: 111-  
473 121.

474 Prah, F. G., and P. G. Coble 1994. Input and behavior of dissolved organic carbon in the  
475 Columbia River estuary, p. 445-450. *In* K. K. Dyer and R. J. Orth (eds.), *Changes in*  
476 *Fluxes in estuaries: Implications from science to management*. Olsen and Olsen,  
477 Fredensborg.

478 Ralison, O. H., A. V. Borges, F. Dehairs, J. J. Middelburg, and S. Bouillon. 2008. Carbon  
479 biogeochemistry of the Betsiboka estuary (north-western Madagascar). *Organic*  
480 *Geochemistry* **39**: 1649-1658.

481 Raymond, P. A., and C. S. Hopkinson. 2003. Ecosystem modulation of dissolved carbon age in a  
482 temperate marsh-dominated estuary. *Ecosystems* **6**: 694-705.

483 Raymond, P. A., and J. E. Bauer. 2001a. DOC cycling in a temperate estuary: a mass balance  
484 approach using natural  $^{14}\text{C}$  and  $^{13}\text{C}$  isotopes. *Limnology and Oceanography* **46**: 655-677.

485 Raymond, P. A., and J. E. Bauer. 2001b. Use of  $^{14}\text{C}$  and  $^{13}\text{C}$  natural abundances for evaluating  
486 riverine, estuarine, and coastal DOC and POC sources and cycling: a review and  
487 synthesis. *Organic Geochemistry* **32**: 469-485.

488 Raymond, P. A., and J. E. Bauer. 2001c. Riverine export of aged terrestrial organic matter to the  
489 North Atlantic Ocean. *Nature* **409**: 497-500.

490 Raymond, P. A., J. E. Bauer, and J. J. Cole. 2000. Atmospheric CO<sub>2</sub> evasion, dissolved inorganic  
491 carbon production, and net heterotrophy in the York River estuary. *Limnology and*  
492 *Oceanography* **45**: 1707-1717.

493 Raymond, P. A., J. E. Bauer, N. F. Caraco, J. J. Cole, B. Longworth, and S. T. Petsch. 2004.  
494 Controls on the variability of organic matter and dissolved inorganic carbon ages in  
495 northeast US rivers. *Marine Chemistry* **92**: 353-366.

496 Raymond, P. A., and J. J. Cole. 2001. Gas exchange in rivers and estuaries: choosing a gas  
497 transfer velocity. *Estuaries* **24**: 312-317.

498 Raymond, P. A., N. F. Caraco, and J. J. Cole. 1997. Carbon dioxide concentration and  
499 atmospheric flux in the Hudson River. *Estuaries* **20**: 381-390.

500 Servais, P., and J. Garnier. 2006. Organic carbon and bacterial heterotrophic activity in the  
501 maximum turbidity zone of the Seine estuary (France). *Aquatic Sciences* **68**: 78-85.

502 Servais, P., A. Barillier, and J. Garnier. 1995. Determination of the biodegradable fraction of  
503 dissolved organic-carbon in waters. *Annales de Limnologie-International Journal of*  
504 *Limnology* **31**: 75-80.

505 Sholkovitz, E. R., E. A. Boyle, and N. B. Price. 1978. Removal of dissolved humic acids and  
506 iron during estuarine mixing. *Earth and Planetary Science Letters* **40**: 130-136.

507 Spencer, R. G. M., J. M. E. Ahad, A. Baker, G. L. Cowie, R. Ganeshram, R. C. Upstill-Goddard,  
508 and G. Uher. 2007. The estuarine mixing behaviour of peatland derived dissolved organic  
509 carbon and its relationship to chromophoric dissolved organic matter in two North Sea  
510 estuaries (U.K.). *Estuarine Coastal and Shelf Science* **74**: 131-144.

- 511 Spiker, E. C. 1980. The behavior of  $^{14}\text{C}$  and  $^{13}\text{C}$  in estuarine water: effects of in situ  $\text{CO}_2$   
512 production and atmospheric exchange. *Radiocarbon* **22**: 647-654.
- 513 Stuiver, M. 1980. Workshop on  $^{14}\text{C}$  data reporting. *Radiocarbon* **22**: 964-966.
- 514 Stuiver, M., and H. A. Polach. 1977. Discussion: reporting of  $^{14}\text{C}$  data. *Radiocarbon* **19**: 355-  
515 363.
- 516 Swaney, D. P., R. W. Howarth, and T. J. Butler. 1999. A novel approach for estimating  
517 ecosystem production and respiration in estuaries: application to the oligohaline and  
518 mesohaline Hudson River. *Limnology and Oceanography* **44**: 1509-1521.
- 519 Taylor, G. T., J. Way, and M. I. Scranton. 2003. Planktonic carbon cycling and transport in  
520 surface waters of the highly urbanized Hudson River estuary. *Limnology and*  
521 *Oceanography* **48**: 1779-1795.
- 522 Uncles, R. J., P. E. Frickers, A. E. Easton, M. L. Griffiths, C. Harris, R. J. M. Howland, R. S.  
523 King, A. W. Morris, D. H. Plummer, and A. D. Tappin. 2000. Concentrations of  
524 suspended particulate organic carbon in the tidal Yorkshire Ouse River and Humber  
525 Estuary. *Science of the Total Environment* **251**: 233-242.
- 526 Van den Meersche, K., P. Van Rijswijk, K. Soetaert, and J. J. Middelburg. 2009. Autochthonous  
527 and allochthonous contributions to mesozooplankton diet in a tidal river and estuary:  
528 integrating carbon isotope and fatty acid constraints. *Limnology and Oceanography* **54**:  
529 62-74.
- 530 Vogel, J. S., D. E. Nelson, and J. R. Southon. 1987. C-14 background levels in an accelerator  
531 mass spectrometry system. *Radiocarbon* **29**: 323-333.

532 Wang, X., R. F. Chen, and G. B. Gardner. 2004. Sources and transport of dissolved and  
533 particulate organic carbon in the Mississippi River estuary and adjacent coastal waters of  
534 the northern Gulf of Mexico. *Marine Chemistry* **89**: 241-256.

535 Williams, P. M. and L. I. Gordon. 1970. Carbon-13 : carbon-12 ratios in dissolved and  
536 particulate organic matter in the sea. *Deep-Sea Research* **17**: 19-27.

537 Zappa, C. J., W. R. McGillis, P. A. Raymond, J. B. Edson, E. J. Hints, H. J. Zemelink, J. W.  
538 H. Dacey, and D. T. Ho. 2007. Environmental turbulent mixing controls on air-water gas  
539 exchange in marine and aquatic systems. *Geophysical Research Letters* **34**: L10601, doi:  
540 10.1029/2006GL028790.

541

542 **TABLE 1.** DOC concentration and isotope data for six WWTPs associated with the lower  
 543 Hudson River Estuary (Griffith et al. 2009). The location of each outfall is shown in Fig. 1.

WWTP	Date sampled	Flow (2005 AVG) (MGD)	DOC ( $\mu\text{M}$ )	$\delta^{13}\text{C}$ DOC (‰)	$\Delta^{14}\text{C}$ DOC (‰)	DOC age (years BP)
WWTP 1	1 August 2006	9.5	nd	nd	nd	nd
WWTP 2	1 August 2006	23	1108	-25.4	nd	nd
WWTP 3	1 August 2006	254	1368	-26.8	-162.5	1364
WWTP 4	14 August 2006	5.3	848	-27.3	-197.3	1707
WWTP 5	14 August 2006	4.6	898	-27.9	-154.5	1290
WWTP 6	14 August 2006	105	548	-25.5	-139.6	1153
average		nd	954	-26.6	-163.5	1379
std deviation		nd	306	1.1	24.4	236

544 nd = not determined

545 MGD = million gallons per day

546 AVG = average

547 WWTP = wastewater treatment plant

548

549 **TABLE 2.** Summary of pCO<sub>2</sub> and chlorophyll *a* data during three longitudinal transects in the  
550 lower Hudson River Estuary (see Figs. 4a and 4b).

Transect	pCO <sub>2</sub> average ( $\mu$ atm)	pCO <sub>2</sub> range ( $\mu$ atm)	chl <i>a</i> average ( $\mu$ g L <sup>-1</sup> )	chl <i>a</i> range ( $\mu$ g L <sup>-1</sup> )
8 June 2005	1000	300 - 1609	nd	nd
19 April 2006	670	587 - 773	4.5	3 - 13
18 July 2006	2059	1028 - 2434	24	16 - 83

551 nd = not determined

552

553

554 **TABLE 3.** Summary of DOC concentration and isotope data during three longitudinal transects  
 555 in the lower Hudson River Estuary (see Figs. 3a - 3c).

Transect	Station	Latitude (decimal degrees)	Longitude (decimal degrees)	Salinity	DOC Concentration ( $\mu\text{M}$ )	$\delta^{13}\text{C}$ DOC (‰)	$\Delta^{14}\text{C}$ DOC (‰)
8 June 2005	1	41.427	-73.986	0	232	-27.2	13
8 June 2005	2	41.277	-73.960	1.4	214	-28.9	31
8 June 2005	3	41.163	-73.905	3.8	176	-29.2	46
8 June 2005	4	41.023	-73.889	5.1	137	-29.7	59
8 June 2005	5	40.813	-73.975	9.2	135	-29.0	nd
8 June 2005	6	40.749	-74.017	12.5	114	-28.8	-59
19 April 2006	1	41.373	-73.956	0.2	216	-27.7	43
19 April 2006	2	41.282	-73.954	0.8	183	-29.7	101
19 April 2006	3	41.197	-73.929	2.7	155	-30.2	89
19 April 2006	4	41.041	-73.886	4.5	117	-29.4	95
19 April 2006	5	40.928	-73.912	7.3	123	-29.5	105
19 April 2006	6	40.830	-73.962	9.3	139	-28.9	91
19 April 2006	7	40.687	-74.041	18.8	103	-25.0	-10
18 July 2006	1	41.385	-73.953	0.2	400	-29.0	57
18 July 2006	2	41.268	-73.971	0.3	274	-26.7	83
18 July 2006	3	41.163	-73.914	0.8	297	-29.0	64
18 July 2006	4	41.038	-73.885	2.4	276	-28.9	70
18 July 2006	5	40.837	-73.957	5.0	242	-29.3	46
18 July 2006	6	40.687	-74.039	14.5	149	-28.6	18

556 nd = not determined

557

558

559 **Figure Legends**

560 **Fig. 1.** Map of the lower Hudson River Estuary. The black curve is a representative transect (19  
561 April 2006) and triangles indicate the location of sampled wastewater treatment plant outfalls.

562 **Fig. 2.** Discharge of the Hudson River at the southern tip of Manhattan (river km 0) was  
563 estimated as 167% of the discharge from the Green Island, NY river gauge (Howarth et al. 1996;  
564 USGS). Our three transects (8 June 2005, 19 April 2006, and 18 July 2006) are shown as circles.

565 **Fig. 3. a)** DOC, **b)**  $\delta^{13}\text{C}$ -DOC, and **c)**  $\Delta^{14}\text{C}$ -DOC mixing curves for three transects in the Hudson  
566 River Estuary where circles are measured values and solid lines represent conservative mixing  
567 scenarios. Landmarks are abbreviated NY (river km 0, New York City), TZ (Tappan Zee  
568 Bridge), and WP (West Point).

569 **Fig. 4. a)**  $\text{pCO}_2$  and **b)** chlorophyll *a* as a function of river kilometer (km 0 is at the southern tip  
570 of Manhattan; see Fig. 1). Landmarks are abbreviated NY (river km 0, New York City), TZ  
571 (Tappan Zee Bridge), and WP (West Point). The dashed line at 380  $\mu\text{atm}$  represents saturation  
572 with atmospheric  $\text{CO}_2$ , and circles indicate the location of discrete sampling sites.

573 **Fig. 5.** Comparing chlorophyll *a* concentrations as measured by a fluorometer in the laboratory  
574 and a flow-through probe while underway. The best linear fit was used to convert high spatial  
575 resolution probe voltages to the chlorophyll *a* concentrations reported in Fig. 4b.

74°00'W 73°40'W

# Lower Hudson River Estuary

41°20'N

41°20'N

West Point →

km 80

WWTP 5

km 60

WWTP 4

← Tappan Zee Bridge

WWTP 1  
WWTP 2

km 40

WWTP 6

George Washington Bridge →

km 20

Manhattan

Long Island Sound

Statue of Liberty →

km 0

WWTP 3



41°00'N

41°00'N

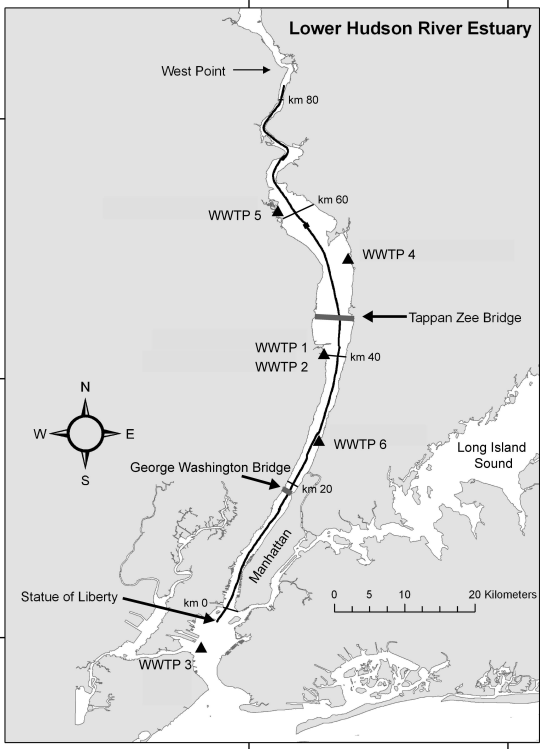


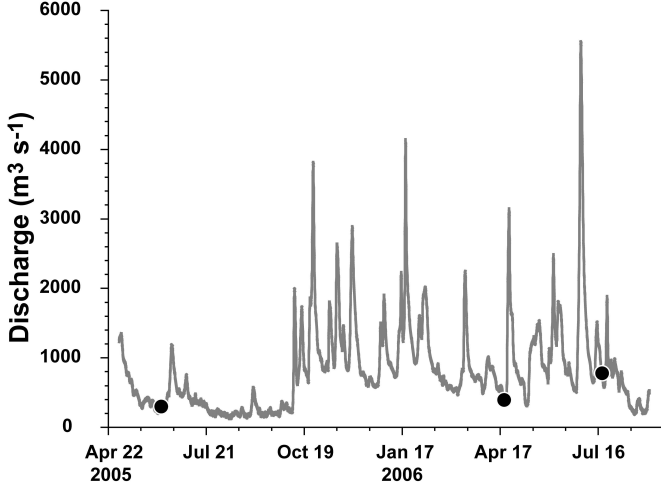
40°40'N

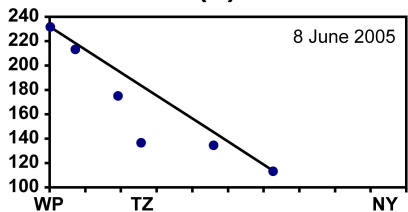
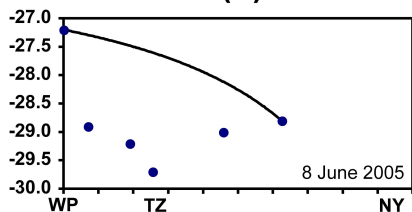
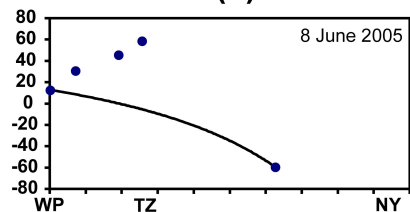
40°40'N

74°00'W

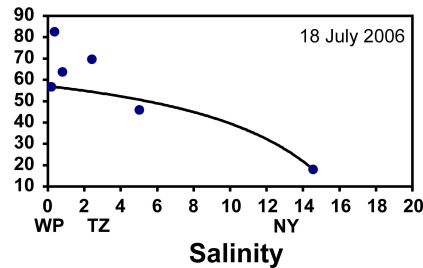
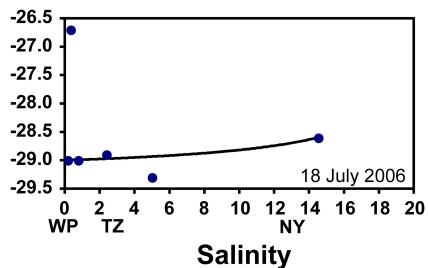
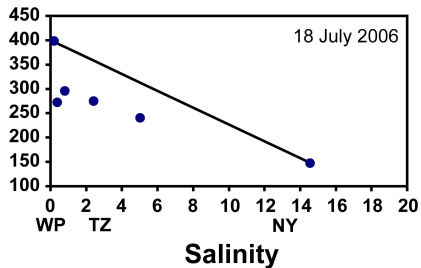
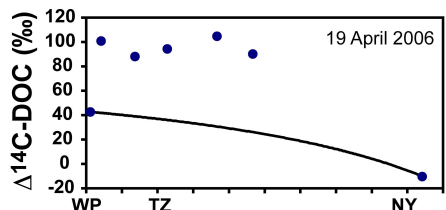
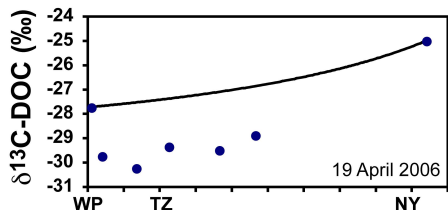
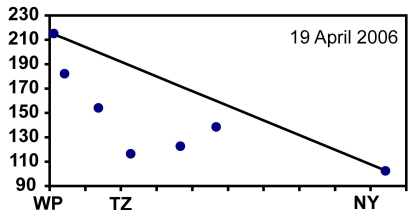
73°40'W





**(a)****(b)****(c)**

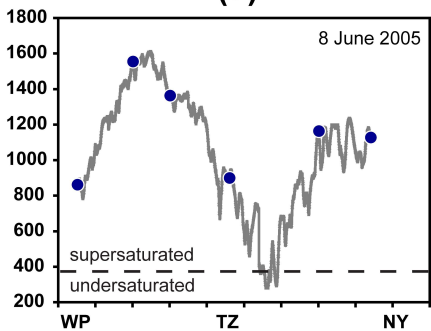
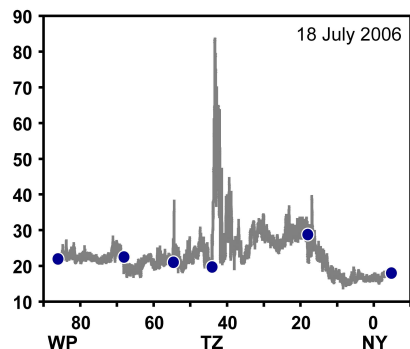
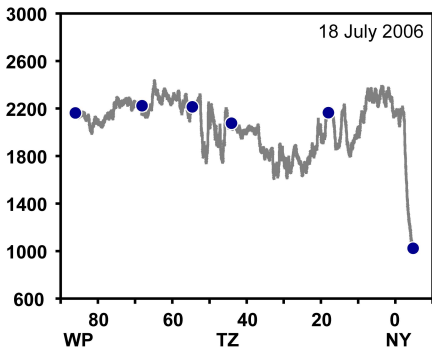
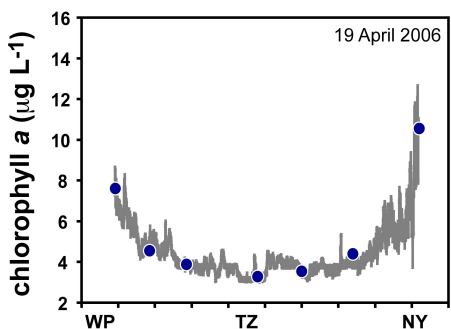
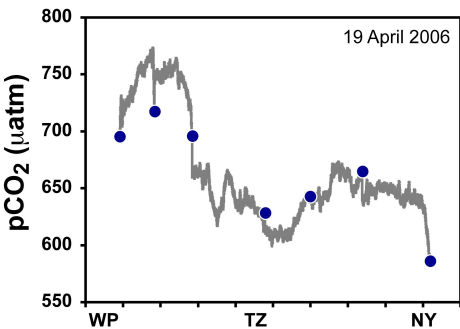
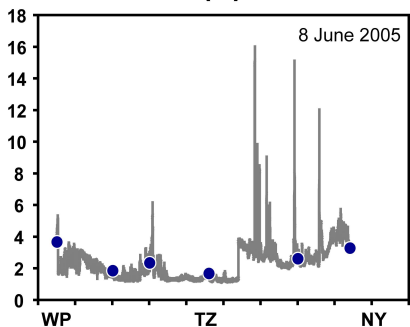
DOC (µM)



Salinity

Salinity

Salinity

**(a)****(b)**

River Kilometer

River Kilometer

